Conformational Changes of the Ca^{2+} Regulatory Site of the Na^+-Ca^{2+} Exchanger Detected by FRET

Michela Ottolia,*† Kenneth D. Philipson,*†‡ and Scott John*‡
*Cardiovascular Research Laboratories, and Departments of †Physiology and ‡Medicine (Cardiology), David Geffen School of Medicine at the University of California, Los Angeles, California 90095-1760

ABSTRACT The Na^+-Ca^{2+} exchanger is a plasma membrane protein expressed at high levels in cardiomyocytes. It extrudes 1 Ca^{2+} for 3 Na^+ ions entering the cell, regulating intracellular Ca^{2+} levels and thereby contractility. Na^+-Ca^{2+} exchanger activity is regulated by intracellular Ca^{2+}, which binds to a region (amino acids 371–508) within the large cytoplasmic loop between transmembrane segments 5 and 6. Regulatory Ca^{2+} activates the exchanger and removes Na^+-dependent inactivation. The physiological role of intracellular Ca^{2+} regulation of the exchanger is not yet established. Yellow (YFP) and cyan (CFP) fluorescent proteins were linked to the NH_2- and CO_2H-termini of the exchanger Ca^{2+} binding domain (CBD) to generate a construct (YFP-CBD-CFP) capable of responding to changes in intracellular Ca^{2+} concentrations by FRET efficiency measurements. The two fluorophores linked to the CBD are sufficiently close to generate FRET. FRET efficiency was reduced with increasing Ca^{2+} concentrations. Titrations of Ca^{2+} concentration versus FRET efficiency indicate a K_D for Ca^{2+} of ~140 nM, which increased to ~400 nM in the presence of 1 mM Mg^{2+}. Expression of YFP-CBD-CFP in myocytes, generated changes in FRET associated with contraction, suggesting that NCX is regulated by Ca^{2+} on a beat-to-beat basis during excitation-contraction coupling.

INTRODUCTION

Cytosolic Ca^{2+} is a ubiquitous regulator that controls cellular processes by setting the activity of many proteins. Among these proteins is the Na^+-Ca^{2+} exchanger (NCX). NCX is a plasma membrane protein particularly abundant in myocardium that uses the energy of the transmembrane Na^+ gradient to extrude Ca^{2+} from the cell after each contraction (Philipson and Nicoll, 2000). During each reaction cycle, NCX transports three Na^+ ions into the cell to extrude one Ca^{2+} ion. By pumping Ca^{2+} out of the cell, the NCX protein plays an important role in cardiac Ca^{2+} homeostasis and contractility.

Structural studies show that NCX has nine transmembrane segments with a large intracellular loop located between transmembrane segments 5 and 6 (Nicoll et al., 1999). This large intracellular loop has multiple regulatory regions. In particular, residues 371–508 form a regulatory Ca^{2+} binding site (Levitsky et al., 1994). Ca^{2+} bound to this site is not transported but activates exchange activity and removes a Na^+-dependent inactivation process (Hilgemann et al., 1992b; Levitsky et al., 1994). The exact Ca^{2+} concentration dependence of the Ca^{2+} regulatory effect is uncertain.

Electrophysiological approaches have determined apparent affinity values ranging from 22 nM (whole cell measurements) to 400 nM (giant excised patches) (Hilgemann et al., 1992a). These conflicting results affect interpretation of the physiological role of Ca^{2+} regulation in cardiac cells. The cytoplasmic Ca^{2+} concentration in a resting cardiac myocyte is ~100 nM. Thus, with an apparent K_D of 22 nM, the Ca^{2+} binding site of the exchanger would be saturated at resting conditions, thereby excluding the possibility of a dynamic tuning effect of Ca^{2+} on the exchanger. In contrast, the lower apparent affinity constant of 400 nM would enable increases in cytoplasmic Ca^{2+} to up-regulate the exchanger during the excitation-contraction coupling cycle.

To characterize the Ca^{2+} dependency of regulation of the exchanger, we isolated the Ca^{2+} binding site of the exchanger and determined Ca^{2+} sensitivity both in vivo and in vitro. To this end, we placed amino acid residues 371–508 (Ca^{2+} binding domain, CBD) between two fluorescent proteins (the yellow YFP and cyan CFP variants of green fluorescent protein) to produce the protein YFP-CBD-CFP. Upon excitation, YFP and CFP act in a concerted manner to give fluorescent resonance energy transfer or FRET. FRET is the nonradiative transfer of energy from a fluorescent donor to another excitable moiety; FRET is well established as a technique to determine protein-protein interactions and intramolecular conformational changes (Stryer, 1978). The efficiency of this reaction is strongly dependent on the distance between the two fluorophores: a small variation in distance can cause large changes in FRET efficiency (Stryer, 1978).

Since the exchanger Ca^{2+} binding domain has been shown to undergo major Ca^{2+}-induced conformational changes (Levitsky et al., 1994), we predicted that upon binding Ca^{2+}, YFP-CBD-CFP would alter conformation causing a change in the distance or angle between the two fluorophores and therefore a change in FRET efficiency.

Submitted April 7, 2004, and accepted for publication May 7, 2004.

Address reprint requests to Kenneth D. Philipson, MRL 3-465, Cardiovascular Research Laboratories, David Geffen School of Medicine at the University of California, Los Angeles, Los Angeles, CA 90095-1760. Tel.: 310-825-7679; E-mail: kphilipson@mednet.ucla.edu.

0006-3495/04/08/899/08 $2.00

doi: 10.1529/biophysj.104.043471

We show that increasing intracellular Ca^{2+} reduces FRET efficiency suggesting a relaxation of the peptide. Finally, we also demonstrate that YFP-CBD-CFP can sense changes in intracellular Ca^{2+} within physiological concentration ranges found in actively contracting neonatal myocytes. These results strongly support a physiological role of secondary regulation of the exchanger by Ca^{2+}.

Our results suggest that it is possible to determine a physiologically important function by examining a protein ''module'' in isolation from its parent: in this case, the core Ca^{2+} binding region of the Na^{+}-Ca^{2+} exchanger.

METHODS

Molecular biology

The CBD of NCX was placed between the donor moiety, cyan fluorescent protein, and the acceptor moiety, yellow fluorescent protein. pEYFP C-1 and pECFP N-1 (Clontech, Palo Alto, CA) were ligated together; an *Nhe*I/*Eco*RI fragment (768 bp) from pEYFP C-1 was inserted into *Nhe*I/EcoR1 digested pECFP N-1 to generate pYFP-CFP. The Ca^{2+} binding domain of the exchanger, amino acid residues 371–508, was amplified with two primers such that the 5′ primer incorporated an *Xho*I restriction site and five codons encoding glycine residues before residue 371 (underlined) (AGATCTC-GAGGCGGCGGCGGCGGCAGTAAGATCTT CTTTGAACAA) and the 3′ primer incorporated five codons encoding glycine residues and an EcoR1 restriction site after residue 508 (underlined) (GCTGGCATCTTTACTTTT-GAGGAGGGAGGAGGAGGAGGAATTCTGCA). The PCR product was subcloned into pYFP-CFP using *Xho*I and *Eco*RI restriction enzymes. The final construct YFP-CBD-CFP was confirmed by sequencing.

Cell culture

HEK293, Hela cells, and rat neonatal cardiac myocytes were grown in 35 mm glass bottom Petri dishes in standard culture medium. Rat neonatal myocytes were prepared as described previously (Mitra and Morad, 1985); 24 h after isolation cardiac myocytes were deprived of serum. Petri dishes were pretreated with either fibronectin (Sigma Chemical, St. Louis, MO) or Cell-Tak (Becton Dickinson Labware, Franklin Lakes, NJ). Transfection of cDNAs was accomplished using GenePORTER (GFTinc., San Diego, CA).

FRET measurements

Data were acquired using a Nikon Eclipse TE300 microscope equipped with a mercury lamp (Nikon, A-G Heinze, Lake Forrest, CA), a 40× oil immersion lens (N.A. 1.2) and the following filter cubes (nm): 1. CFP cube (CFP_F): excitation (EX) 436 ± 20, emission (EM) 480 ± 40, dichroic 455 (longpass, DCLP); 2. YFP cube (YFP_F): EX 500 ± 20, EM 535 ± 30, DCLP 515; FRET cube ($FRET_F$): EX 436 ± 20, EM 535 ± 30, DCLP 455 (Chroma Technologies, Rockingham, VT). Alternatively, LEDs (Light Emitting Diodes, Lumileds; San Jose, CA) were used as light sources, two emitting at 455 ± 20 nm (royal blue) and one emitting at 505 ± 15 nm (cyan). The royal blue lights were placed in front of the CFP and FRET filter, whereas the cyan light was located in front of the YFP filter; LEDs were controlled by the camera driven shutter. This setup eliminated the fluctuations typically associated with a mercury lamp. Experiments were performed at room temperature.

Steady-state FRET

Sequential images were captured with a SPOTII digital camera (Diagnostic, Sterling Heights, MI). Control experiments confirm that correction factors values for donor (R_D) and acceptor (R_A) (measured as described in the results) were independent of level of expression. R_A and R_D were found to be 0.54 ± 0.01 ($n = 12$) and 0.73 ± 0.01 ($n = 15$), respectively. These correction factors were utilized to determine the true FRET signal indicated as $FRET^C$ and measured as follows: $FRET^C = FRET_F - R_D \times CFP_F - R_A \times YFP_F$, where $FRET_F$, CFP_F, and YFP_F indicate the type of filter with which the light was acquired from a cell expressing both fluorophores. Cells were illuminated using the mercury lamp. Images were analyzed with the National Institutes of Health Scion Image Program and background was subtracted before FRET calculations. Before the experiment, external medium was replaced with PBS.

FRET efficiency was quantified using the acceptor photobleaching approach (Stryer, 1978; Llopis et al., 2000). For these measurements, wide-field illumination was obtained using the LED lights. YFP photobleaching was completed after ~15 min of constant illumination (YFP_F). CFP emission images were acquired before and after YFP photobleaching using the CFP_F. Images were analyzed by quantifying the amount of fluorescence inside the cell. These values were used to determined FRET efficiency (E), calculated as follow: $E = 1 - I_{CFPb}/I_{CFPa}$, where I is the intensity of CFP emission before (CFP_b) and after (CFP_a) YFP photobleaching.

Control cells were maintained in the presence of PBS, whereas cells in 0 Ca^{2+} were incubated in 160 mM MOPS, 1 mM EGTA, 5 μM ionomycin pH 7.4 (adjusted with KOH) for ~10 min prior experiment.

Real time FRET

Measurements were performed using the MultiSpec Micro-Imager system from Optical Insight (Santa Fe, NM) that allows monitoring of CFP and YFP fluorescence emissions simultaneously. The ratio between YFP and CFP emission is then calculated as an indicator of FRET efficiency. The MultiSpec Micro-Imager is directly attached to the microscope and is equipped with a 505 nm long-pass dichroic filter used to separate the CFP signal from the YFP signal, a CFP emission filter (480 ± 30 nm) and an YFP emission filter (535 ± 40 nm). The excitation filter was 436 ± 20 nm. Images were captured with a fast high-resolution digital camera (Cool-SNAP-fx 12bit Cooled Monochrome Digital Camera, Roper Scientific, Tucson, AZ) and acquired in a PC using the MetaFluor6.1 Fluorescence ratio imaging system (Universal Imaging Corporation, Downingtown, PA). For all experiments only cells with nonsaturating levels of fluorescence are used. Cells were maintained in Tyrode's solution supplemented with 1.8 mM $CaCl_2$ (pH = 7.4).

In vitro FRET measurements

HEK293 cells were cultured in 100 × 20 mm regular culture dishes and transfected with 5 μg DNA. Two to 3 days after transfection, cells were rinsed once with a solution containing 160 mM MOPS, 1 mM EGTA, adjusted to pH 7.2 with KOH and then solubilized using 0.5% Triton X-100, dissolved in 2 ml of the same buffer. After centrifugation, the supernatant was collected and placed in a quartz cuvette mounted in a spectrofluorometer (Photon Technology International, Model C-44/2000, Lawrenceville, NJ). CFP and YFP emission spectra were obtained by exciting at 434 nm and measuring emission between 460–600 nm. Both excitation and emission slits were set at 4 nm.

For ratio measurements, samples were excited at 434 nm and emission was measured at 472 and 524 nm. $CaCl_2$ was added directly to the cuvette equipped with a magnetic stir bar. After addition of Ca^{2+}, a shift of 0.01–0.02 pH units was measured at the end of the experiment. Control experiments using cytoplasmic CFP and YFP show that this change in pH did not affect the spectra of the fluorophores and did not significantly alter the affinity of EGTA for Ca^{2+}, since the replacement of EGTA with 1 mM BAPTA, a less pH sensitive calcium buffer, did not modify the results (not shown).

Free [Ca^{2+}] was calculated using the MAXC program.

RESULTS

Previous studies have demonstrated that the Na^+-Ca^{2+} exchanger has a Ca^{2+} regulatory binding site, which activates the exchanger (DiPolo, 1979; Hilgemann, 1992a). Biochemical evidence localized this regulatory site to lie within the large cytoplasmic loop of the exchanger, specifically between residues 371 and 508 (Levitsky et al., 1994). This region was shown to undergo substantial change in conformation upon the binding of Ca^{2+}, as indicated by a shift in electrophoretic mobility during SDS-PAGE in the presence or absence of Ca^{2+} (Levitsky et al., 1994). These results provided the rational for creating a system to noninvasively monitor these movements in vivo and to determine the range of Ca^{2+} concentrations required to produce conformational changes. To achieve this goal, we constructed a peptide consisting of the CBD of the exchanger (amino acid residues 371–508) with the NH_2- and CO_2H-termini linked to YFP and CFP (YFP-CBD-CFP) (Fig. 1 *A*), respectively. This construct is analogous to a well characterized Ca^{2+}-indicator protein consisting of CFP-calmodulin-calmodulin binding peptide-YFP, known as Cameleon (Miyawaki et al., 1997). Binding of Ca^{2+} to the Cameleon produces an increase in FRET efficiency indicating a shift in the protein to a more compact state in the presence of Ca^{2+}.

Detection of FRET from YFP-CBD-CFP

To determine if the fluorophores linked to the CBD were sufficiently close to generate FRET, we expressed YFP-CBD-CFP in mammalian cells and assessed FRET by using both the three cubes method and the acceptor photobleaching technique (Stryer, 1978; Sorkin et al., 2000; Erickson et al., 2001). Fig. 1 *B* shows HEK293 cells expressing YFP-CBD-CFP and the corresponding corrected FRET ($FRET^C$) examined with the three cubes method. Briefly, $FRET^C$ was obtained by using three filters indicated as CFP, YFP, and FRET. The CFP and YFP filters allow excitation and detection of light from the CFP and YFP fluorophores, respectively. The FRET filter is a hybrid filter, which permits excitation of the donor (CFP) and detection of light from the acceptor (YFP). Ideally, any signal detected through the FRET filter would originate from transfer of energy from CFP to YFP and therefore represent FRET. However, the emission spectra of CFP and YFP partially overlap, and the emitted light measured through the FRET filter is contaminated by the fluorescence due to the direct excitation of both fluorophores. To dissect these components (Sorkin et al., 2000; Erickson et al., 2001) CFP and YFP were expressed separately and for each fluorophore, we divided the emission from the FRET filter by the emission measured with either the CFP (for CFP) or YFP (for YFP) filters. This correction factor (R) is independent of the amount of fluorescent protein and was utilized to determine the true FRET signal ($FRET^C$; see Methods). As is shown in Fig. 1 *B*, we successfully detected FRET generated by both YFP-CBD-CFP and Cameleon. To corroborate our findings, we coexpressed cytoplasmic CFP and YFP in the same cells and, as expected, no FRET was detected.

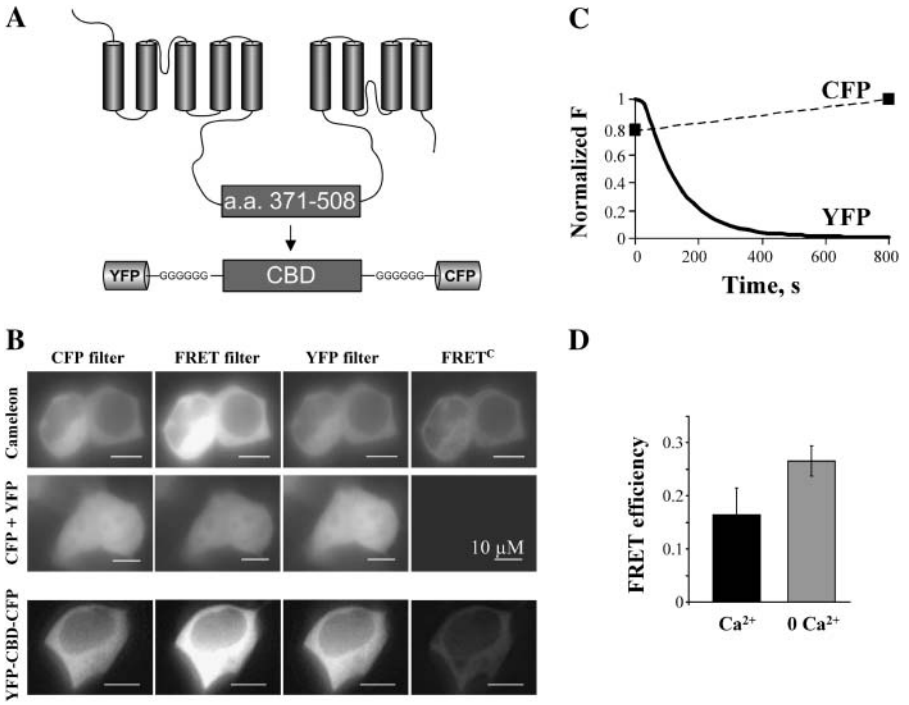

FIGURE 1 FRET determination using the three cubes and the acceptor photobleaching techniques. (*A*) Schematic representation of the Na^+-Ca^{2+} exchanger topology and the YFP-CBD-CFP construct. (*B*) An example of assessment of FRET using the three cubes method for the following cytoplasmic constructs: cameleon, a well-characterized construct generating Ca^{2+}-dependent FRET (Miyawaki et al., 1997); CFP and YFP coexpressed; and the exchanger Ca^{2+} binding domain linked to YFP and CFP (YFP-CBD-CFP). The images were acquired with the CFP, YFP, and FRET filters and $FRET^C$ was calculated as described in the text. Notice the lack of FRET in cells expressing cytoplasmic CFP and YFP. (*C*) Example of increase in the CFP emission after YFP photobleaching in a cell expressing YFP-CBD-CFP. CFP images were acquired immediately before and after YFP photobleaching. After YFP photobleaching, achieved with maximal excitation at 500 nm for 800 s, CFP emission increased by 22%, demonstrating the presence of FRET. (*D*) FRET efficiency was determined using the increase in CFP emission (see Methods). Cells incubated with 5 μM ionomycin in the presence of 1 mM EGTA (0 Ca^{2+}) show an increase in FRET efficiency, as compared to untreated cells (Ca^{2+} ~100 nM). FRET efficiency values are 0.27 ± 0.03 ($n = 7$) and 0.16 ± 0.05 ($n = 3$) ($p < 0.05$), respectively. The result indicates that low Ca^{2+} favors FRET.

FRET was also determined by acceptor photo bleaching (YFP). This method relies on the concept that when FRET occurs part of the energy of excited CFP is transferred to YFP resulting in decreased in CFP emission (Stryer, 1978). This energy transfer is eliminated by bleaching of YFP and leads to an increase in CFP emission. Fig. 1 *C* illustrates the time course of YFP photobleaching, obtained with a constant illumination of the cells at 500 ± 20 nm for ~15 min, and the corresponding increase in CFP emission of YFP-CBD-CFP expressed in HEK293 cells. CFP and YFP values were normalized to their own maximum. After complete YFP bleaching, the CFP emission increased by 22%, indicative of FRET occurring between the two fluorophores. Photobleaching of YFP in cells coexpressing cytoplasmic CFP and YFP did not modify CFP emission (not shown).

The increase in CFP emission was used to determine the efficiency with which energy was transferred from CFP to YFP (FRET efficiency; see Methods), which is dependent on fluorophore proximity (Stryer, 1978). The average value of FRET efficiency obtained from cells expressing YFP-CBD-CFP and incubated in PBS was lower than that in cells treated with 5 μM ionomycin in the presence of 1 mM EGTA to chelate cytoplasmic Ca^{2+} (see *lower panel*, Fig. 1 *D*). The result indicates that cytoplasmic Ca^{2+} drives the exchanger Ca^{2+} binding domain into a conformation that decreases FRET.

The Ca^{2+} binding region of the exchanger senses physiological Ca^{2+} concentrations

Since the three cubes and the acceptor photobleaching methods are only useful to determine FRET under steady-state conditions, we utilized a ratiometric approach to monitor changes in FRET during interventions. When FRET occurs, excitation of CFP causes YFP emission at the expense of CFP emission. Hence, the YFP/CFP fluorescence ratio is a measure of FRET efficiency. Fig. 2 shows how the CFP and YFP emission and the corresponding YFP/CFP ratio value changed upon addition of 10 μM carbachol to the external solution of HeLa cells expressing YFP-CBD-CFP and the muscarinic receptor M1. Activation of M1 by carbachol creates a transient increase in cytoplasmic Ca^{2+} (Felder, 1995), which led to a decrease in FRET. As shown in the right panel of Fig. 2, HeLa cells coexpressing cytoplasmic CFP, YFP, and M1 receptor do not show any change in the FRET ratio value, corroborating the specificity of the effect.

To determine the range of Ca^{2+} concentrations to which YFP-CBD-CFP responded, the construct was expressed in HEK293 cells and then used for in vitro studies. After detergent lysis of the cells in an EGTA-buffered, low Ca^{2+} solution, the FRET ratio of YFP-CBD-CFP was monitored in a spectrofluorimeter after additions of Ca^{2+}. Fig. 3 *A* shows the emission spectra of solubilized YFP-CDB-CFP before and after addition of 1 μM Ca^{2+}. Ca^{2+} induced a decrease in the FRET ratio value. The changes in FRET were plotted versus free Ca^{2+} concentration and the values were fit to the Hill function to determine the apparent dissociation constant (K_D). As shown in Fig. 3 *B*, the fit of the averages from 8 different experiments gave a K_D for Ca^{2+} of 140 nM and a Hill coefficient of 2.9. Since Mg^{2+} competes for Ca^{2+} at the regulatory site (Levitsky et al., 1994; Wei et al., 2002), we also measured the K_D for Ca^{2+} in the presence of 1 mM Mg^{2+} ($n = 4$). The apparent Ca^{2+} affinity for FRET was shifted to 383 nM. However, Mg^{2+} by itself did not evoke any changes in FRET up to a concentration of 3 mM (not shown), perhaps suggesting that Mg^{2+} can interact with the Ca^{2+}-binding site of the exchanger but is incapable of generating a detectable conformation change.

GFP molecules can potentially form dimers (Tsien, 1998), and we investigated the possibility of intermolecular FRET

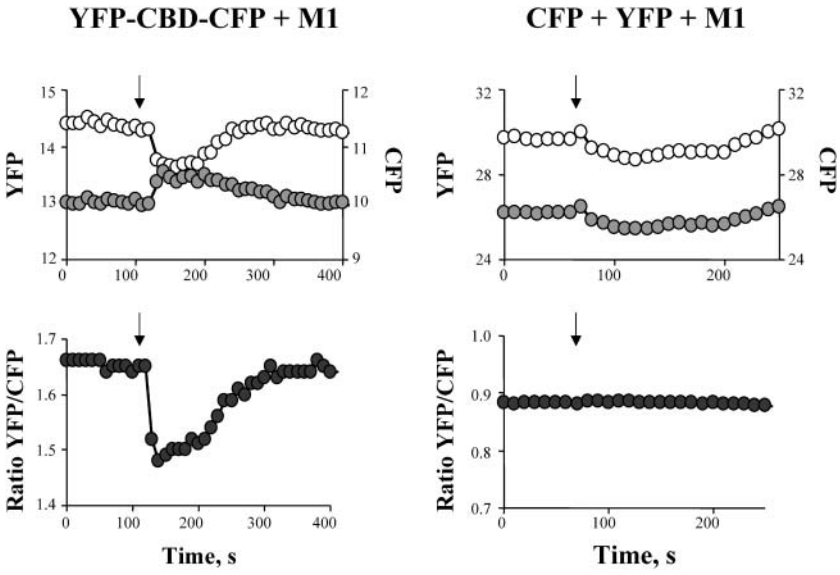

FIGURE 2 Ca^{2+} decreases FRET: effect of changes in intracellular Ca^{2+} on CFP (*open circles*) and YFP (*shaded circles*) emissions (*top*) and corresponding YFP/CFP ratio (*bottom*), from HeLa cells expressing YFP-CBD-CFP (*right*) or CFP + YFP (*left*) in the presence of the muscarinic receptor M1. Cytoplasmic Ca^{2+} was increased by activation of the muscarinic receptor M1 with the agonist carbachol. The YFP/CFP ratio of cells expressing YFP-CBD-CFP significantly decreased with the induced rise in intracellular Ca^{2+} concentration, whereas the ratio from cells expressing cytoplasmic CFP and YFP remained constant. Arrows indicate the addition of 10 μM carbachol to the external Tyrode's solution.

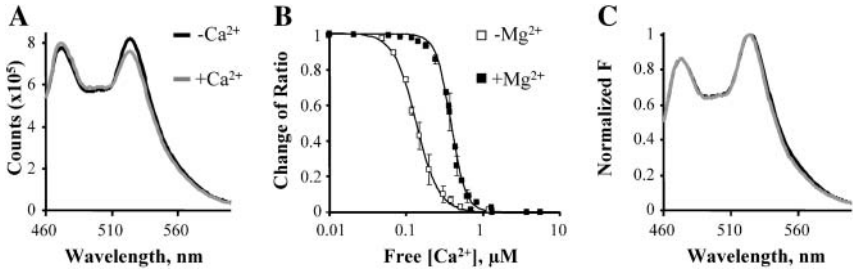

FIGURE 3 Fluorescence properties of YFP-CBD-CFP in vitro. (*A*) Emission spectra of solubilized YFP-CBD-CFP (excited at 434 nm) in the absence or presence of 1 μM free Ca^{2+}. Ca^{2+} addition induced a decrease in the YFP/CFP ratio without altering the spectral properties of YFP-CBD-CFP. (*B*) Changes in the emission ratio versus Ca^{2+} concentration. Each point represents the average of eight experiments. Emission ratios were normalized to the value obtained in the absence of Ca^{2+} and fit to the Hill function $(1/1 + ([Ca^{2+}]/K_D)^n)$, where K_D is the dissociation constant and n the Hill coefficient. The Ca^{2+} titration curve has a K_D of 140 nM and a Hill coefficient of 2.9. Addition of 1 mM Mg^{2+} (■) induced a shift in the K_D value to 383 nM. (*C*) Emission spectra of YFP-CBD-YFP (excited at 434 nm) before and after an eightfold dilution. Both spectra were normalized to emission at 514 nm.

induced by the dimerization of YFP-CBD-CFP. The efficiency of dimerization of adjacent molecules is dependent on protein concentration. Fig. 3 *C* shows that this is not the case, since the ratio between YFP/CFP was not affected by a eightfold dilution of YFP-CBD-CFP. The result indicates that FRET occurs exclusively between CFP and YFP of the same molecule and measures the intrinsic movements of the connecting moiety; i.e., it gives an indication of the movements of the Ca^{2+} binding domain of the Na^+-Ca^{2+} exchanger.

FRET is altered by mutations known to reduce the Ca^{2+} affinity of the exchanger

Previous studies have shown that point mutations (D447V and D498I) within the Ca^{2+} binding domain of the exchanger decreased Ca^{2+} affinity (Matsuoka et al., 1995). Using FRET, we measured the Ca^{2+} dependency of YFP-CBD-CFP with either D447 or D498 mutated. As shown in Fig. 4 *A*, mutation of the aspartate at position 447 to valine shifted the Ca^{2+} affinity. The response to Ca^{2+} was best fit with a linear combination of two Hill functions with apparent Ca^{2+} affinities of 1.2 and 2.5 μM and relative contributions of 76% and 24%, respectively. The mutation also decreased the total change in FRET (ΔFRET) by 13% compared to WT (Fig. 4 *B*). Replacement of aspartate 498 with an isoleucine also exposed two Ca^{2+} binding sites with apparent affinities of 1.2 and 130 μM (relative contributions were 59% and 41%, respectively (Fig. 4 *A*) and reduced the total change in FRET by 29% (Fig. 4 *B*).

These data suggest that mutation of these residues not only decreases Ca^{2+} affinity but also partially hinders the rearrangement of the protein after the binding of Ca^{2+}. The double mutant D447V-D498I showed a Ca^{2+} insensitive YFP/CFP ratio, although a full-length exchanger with this double mutation retains weak Ca^{2+} regulation (Levitsky et al., 1994; Matsuoka et al., 1995).

The exchanger Ca^{2+} binding domain undergoes conformational changes during excitation-contraction coupling

One objective of our study was to determine if the Ca^{2+} binding site of the Na^+-Ca^{2+} exchanger could sense changes in cytoplasmic Ca^{2+} during each contraction cycle. To address this question, we expressed YFP-CBD-CFP in rat neonatal cardiac myocytes and monitored changes in FRET during spontaneous contractions. Three to four days after DNA transfection, media was replaced with regular Tyrodes solution and the spontaneous contractions of myocytes expressing YFP-CBD-CFP were monitored at room temperature. Fast acquisition of simultaneous images of CFP and YFP revealed a change in the YFP/CFP fluorescence ratio, which correlated with myocyte contraction. Consistent with our previous observations, the YFP/CFP fluorescence ratio was maximal during relaxation and decreased significantly

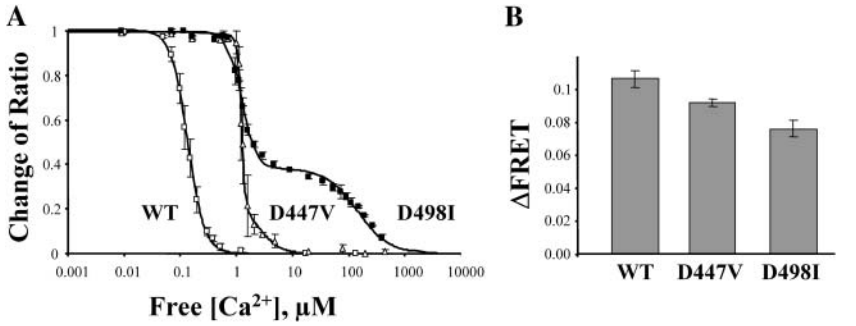

FIGURE 4 Mutation of aspartates 447 and 498 alters Ca^{2+} dependency of FRET signals. (*A*) Changes in FRET value versus free Ca^{2+} concentrations for WT and mutants D447V and D498I. Emission ratios were normalized to the value obtained in the absence of Ca^{2+} and fitted to a single Hill function for wild-type and to the sum of two Hill functions for mutants D447V and D498I. K_D values are WT, 140 nM; D447V, 1.2 and 2.5 μM; and D498I, 1.2 and 130 μM. Each point is the mean of eight experiments for WT, five experiments for D497V, and six experiments for D498I. (*B*) The graph shows the total change in FRET signal (ΔFRET) for the WT and mutants D447V and D498I. Values are WT = 0.109 ± 0.005 (n = 8), D447V = 0.091 ± 0.003 (n = 5), and D498I = 0.075 ± 0.005 (n = 5). ΔF is the difference between the YFP/CFP value in 0 Ca^{2+} and YFP/CFP value in presence of high $[Ca^{2+}]$.

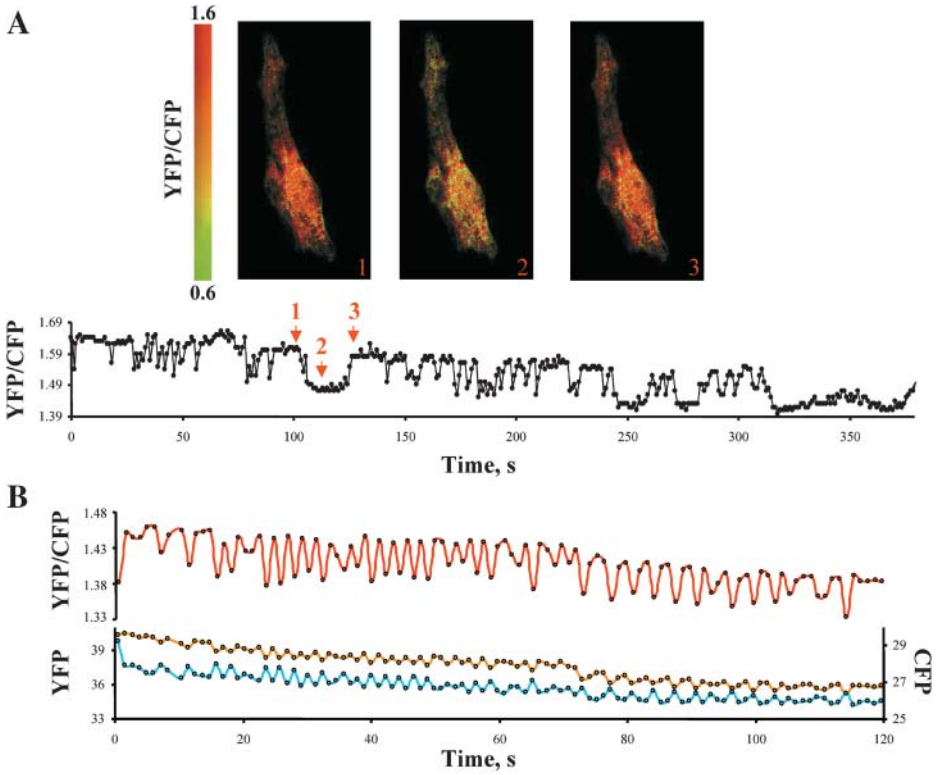

FIGURE 5 The Ca^{2+} binding site of the exchanger can sense changes in Ca^{2+} during excitation-contraction coupling. (*A*) An example of rat neonatal cardiomyocytes expressing YFP-CBD-CFP and the corresponding changes in YFP/CFP ratio during spontaneous activity of the myocytes. Arrows indicate the time when the images were acquired. Myocytes were kept in Tyrode's solution at room temperature and fluorescence was monitored each second. The vertical bar indicates the YFP/CFP ratio value in pseudocolor. The decrease in the ratio of YFP/CFP correlates with myocyte contraction (not shown). (*B*) Another example of changes in YFP/CFP ratio during spontaneous contractions of a different neonatal cardiac myocyte. In this case, the contractions were faster. The lower panel shows how the CFP and YFP emissions changed during time. Changes in YFP/CFP values were due to simultaneous and opposite oscillations in CFP and YFP emissions. Images were acquired every second.

during contractions when cytoplasmic Ca^{2+} was elevated (Fig. 5). Prolonged decreases in FRET correlated with protracted states of contractions (Fig. 5 *A*). Another example of a contracting cardiac myocyte is shown in Fig. 5 *B*. In this case the myocyte displayed fast twitches, which were associated with rapid changes in the FRET signal. The corresponding changes in both CFP and YFP emission are also shown for this myocyte and, as expected, opposite changes in YFP and CFP emission were associated with FRET oscillations. Similar results were observed in an additional 22 myocytes. The data indicate that the regulatory Ca^{2+} binding site of the exchanger responds to changes in Ca^{2+} that occur during excitation-contraction coupling. Control experiments monitoring the fluorescence of myocytes expressing cytoplasmic CFP and YFP or mutants D498I and D447V demonstrated no changes in FRET with contraction (data not shown).

DISCUSSION

The regulatory CBD of the Na^+-Ca^{2+} exchanger consists of amino acid residues 371 to 508 (Levitsky et al., 1994). The affinity of the CBD for Ca^{2+} has been extensively studied using techniques such as $^{45}Ca^{2+}$ overlay, radioisotopic flux, and electrophysiology. These techniques have characterized the general properties of Ca^{2+}-induced regulation of the Na^+-Ca^{2+} exchanger. Nevertheless, Ca^{2+} regulation is difficult to study in intact myocytes, and an accurate in vivo value for Ca^{2+} affinity has proven to be elusive with values ranging from 20–400 nM (Miura and Kimura, 1989; Hilgemann et al., 1992a; Reeves and Condrescu, 2003). Problems have included experimental limitations such as difficulties in controlling intracellular Ca^{2+} and measuring exchanger activity, lack of specific inhibitors of Na^+-Ca^{2+} exchange, and partial overlap of the affinity curves for transported and regulatory Ca^{2+}. In our study, this issue was addressed using a noninvasive optical approach to determine the range of cytoplasmic Ca^{2+} needed to activate the Na^+-Ca^{2+} exchanger in living cells. By linking YFP and CFP fluorophores to the NH_2- and CO_2H-termini of the CBD of the exchanger, conformational changes of the protein were translated into changes in FRET, enabling the selective study of CBD in vitro and in vivo in contracting myocytes.

First, we determined the presence of FRET between the two fluorophores linked to the CBD by using two well established independent techniques: the three cubes method (Sorkin et al., 2000; Erickson et al., 2001) and acceptor photobleaching (Llopis et al., 2000). Both techniques demonstrated that YFP-CBD-CFP expressed in mammalian cells generates FRET. To determine if FRET changed with Ca^{2+}, we coexpressed YFP-CBD-CFP with the muscarinic receptor M1. Activation of M1 leads to release of Ca^{2+} from internal stores. Addition of carbachol, a M1 agonist, caused a rapid decrease in FRET; this reduction was transient, as Ca^{2+} is resequestered into the endoplasmic reticulum. These data indicate that the Ca^{2+} binding site of the Na^+-Ca^{2+} exchanger can sense variations in cytoplasmic Ca^{2+} and that binding of Ca^{2+} induces a change in the conformation of

the CBD. The Ca^{2+}-dependent decrease in FRET could potentially be due to a conformational change of the CBD moving the CFP and YFP further apart or changing the orientation of the two fluorophores with respect to one another. A combination of these two mechanisms may also be occurring. Our results cannot discriminate between these possibilities. However, we favor the first interpretation since both CFP and YFP were linked to the Ca^{2+} binding domain by a series of glycines that likely confers flexibility to the orientation of the fluorophores. Interestingly, YFP-CBD-CFP shows a reduction in FRET upon Ca^{2+} binding, a behavior opposite to that observed with Cameleon, a fluorescent Ca^{2+} indicator that increases FRET efficiency upon binding Ca^{2+}.

To determine the sensitivity of the regulatory Ca^{2+} binding site for Ca^{2+}, we performed in vitro measurements. The FRET efficiency of expressed YFP-CBD-CFP from solubilized cells was assessed as a function of Ca^{2+} concentration. The Ca^{2+} needed to cause a 50% reduction in FRET was ~140 nM in the absence of Mg^{2+} and ~400 nM in the presence of 1 mM Mg^{2+}. The rightward shift of the FRET Ca^{2+} affinity in the presence of Mg^{2+} corroborates previous studies (Levitsky et al., 1994; Wei et al., 2002) showing competition between the two ions for the Ca^{2+} regulatory site.

In sum, these results imply that a majority of Na^+-Ca^{2+} exchangers are in an inactivated state at resting Ca^{2+} concentrations (~100 nM) and that small increases in cytoplasmic Ca^{2+} content could have a large effect on Na^+-Ca^{2+} exchanger activity, assuming that the Ca^{2+} affinity of the CBD reflects that of the intact exchanger. Activation of the exchanger would be maximal by ~1 μM internal Ca^{2+}.

Two clusters of aspartate residues located within the exchanger Ca^{2+} binding domain have previously been shown to be important for binding. Point mutations at either of these sites alter Ca^{2+} affinity as measured biochemically by $^{45}Ca^{2+}$ overlay (Levitsky et al., 1994) and functionally by the giant excised patch technique (Matsuoka et al., 1995). Mutation of residues D447 or D498 lowered the apparent affinity for Ca^{2+} from 0.4 to 1.8 and 1.4 μM, respectively (Matsuoka et al., 1995). These same mutations also cause a rightward shift of the Ca^{2+} dependency when studied with the $^{45}Ca^{2+}$ overlay technique (Levitsky et al., 1994). We investigated the changes in FRET associated with Ca^{2+} binding for the mutants D447V, D498I, and the double mutant D447V/D498I. Our data show that replacement of aspartate 447 with a valine altered the Ca^{2+} binding curve and revealed the presence of low and high affinity sites with K_D values of 1.2 and 2.4 μM, respectively. The biphasic form of the Ca^{2+} titration was more accentuated by the replacement of aspartate 498 with valine since this mutation produced a drastic rightward shift of the low affinity site ($K_D > 100$ μM). The presence of a biphasic response of FRET to Ca^{2+} could represent the equilibrium of the protein between multiple states with different FRET efficiencies. In addition to alter Ca^{2+} affinity, significant reductions (10–30%) in ΔFRET was also observed with both mutants. Finally, a complete lack of change in FRET was observed when the two mutations were combined. The findings corroborate the importance of these residues in Ca^{2+} regulation of the exchanger.

To determine if activation of the Na^+-Ca^{2+} exchanger by the binding of regulatory Ca^{2+} could occur during excitation-contraction coupling, we expressed YFP-CBD-CFP in neonatal cardiac myocytes and measured the change in FRET upon contraction. Our data clearly show oscillations in the YFP/CFP fluorescence ratio associated with myocyte contraction. FRET was maximal during relaxation and decreased during contraction. The changes in fluorescence were fast enough to track each contraction of the myocyte. The changes in FRET were not motion artifacts, as FRET changes were not detected when mutants with reduced Ca^{2+} affinity (D447V and D498I) were expressed in the myocytes.

In summary, the results demonstrate that the Ca^{2+} regulatory site of the Na^+-Ca^{2+} exchanger can sense changes in Ca^{2+} within the physiological range and that the rearrangement of the protein upon the binding of Ca^{2+} is fast enough to follow the rapid variations in cytoplasmic Ca^{2+} that occur during excitation-contraction coupling. The same Ca^{2+}-induced conformational changes that cause changes in FRET presumably also lead to activation of exchange activity. A caveat to our conclusions results from the fact that the data were obtained using a soluble form of the CBD that may not have identical characteristics to the Ca^{2+} binding site on the full length, intact exchanger protein. Also, Ca^{2+} levels in the subsarcolemmal environment where the CBD would normally be located may be different from those in the bulk cytoplasm. Further work to investigate these issues is underway.

This work was supported by Beginning Grant-In-Aid (0365104Y) from the American Heart Association Western States Affiliate (M.O.), by National Institutes of Health grant HL49101 (K.D.P.), and by the Laubish Fund (S.J.).

REFERENCES

DiPolo, R. 1979. Calcium influx in internally dialyzed squid giant axons. *J. Gen. Physiol.* 73:91–113.

Erickson, M. G., B. A. Alseikhan, B. Z. Peterson, and D. T. Yue. 2001. Preassociation of calmodulin with voltage-gated Ca^{2+} channels revealed by FRET in single living cells. *Neuron.* 31:973–985.

Felder, C. C. 1995. Muscarinic acetylcholine receptors: signal transduction through multiple effectors. *FASEB J.* 9:619–625.

Hilgemann, D. W., A. Collins, and S. Matsuoka. 1992a. Steady-state and dynamic properties of cardiac sodium-calcium exchange. Secondary modulation by cytoplasmic calcium and ATP. *J. Gen. Physiol.* 100:933–961.

Hilgemann, D. W., S. Matsuoka, G. A. Nagel, and A. Collins. 1992b. Steady-state and dynamic properties of cardiac sodium-calcium exchange. Sodium-dependent inactivation. *J. Gen. Physiol.* 100:905–932.

Levitsky, D. O., D. A. Nicoll, and K. D. Philipson. 1994. Identification of the high affinity Ca^{2+}-binding domain of the cardiac $Na+$-Ca^{2+} exchanger. *J. Biol. Chem.* 269:22847–22852.

Llopis, J., S. Westin, M. Ricote, Z. Wang, C. Y. Cho, R. Kurokawa, T. M. Mullen, D. W. Rose, M. G. Rosenfeld, R. Y. Tsien, C. K. Glass, and J. Wang. 2000. Ligand-dependent interactions of coactivators steroid receptor coactivator-1 and peroxisome proliferator-activated receptor binding protein with nuclear hormone receptors can be imaged in live cells and are required for transcription. *Proc. Natl. Acad. Sci. USA.* 97:4363–4368.

Matsuoka, S., D. A. Nicoll, L. V. Hryshko, D. O. Levitsky, J. N. Weiss, and K. D. Philipson. 1995. Regulation of the cardiac Na^{+}-Ca^{2+} exchanger by Ca^{2+}. Mutational analysis of the Ca^{2+}-binding domain. *J. Gen. Physiol.* 105:403–420.

Mitra, R., and M. Morad. 1985. A uniform enzymatic method for dissociation of myocytes from hearts and stomachs of vertebrates. *Am. J. Physiol.* 249:H1056–H1060.

Miura, Y., and J. Kimura. 1989. Sodium-calcium exchange current. Dependence on internal Ca and Na and competitive binding of external Na and Ca. *J. Gen. Physiol.* 93:1129–1145.

Miyawaki, A., J. Llopis, R. Heim, J. M. McCaffery, J. A. Adams, M. Ikura, and R. Y. Tsien. 1997. Fluorescent indicators for Ca^{2+} based on green fluorescent proteins and calmodulin. *Nature.* 388:882–887.

Nicoll, D. A., M. Ottolia, L. Lu, Y. Lu, and K. D. Philipson. 1999. A new topological model of the cardiac sarcolemmal $Na+$-Ca^{2+} exchanger. *J. Biol. Chem.* 274:910–917.

Philipson, K. D., and D. A. Nicoll. 2000. Sodium-calcium exchange: a molecular perspective. *Annu. Rev. Physiol.* 62:111–133.

Reeves, J. P., and M. Condrescu. 2003. Allosteric activation of sodium-calcium exchange activity by calcium: persistence at low calcium concentrations. *J. Gen. Physiol.* 122:621–639.

Sorkin, A., M. McClure, F. Huang, and R. Carter. 2000. Interaction of EGF receptor and grb2 in living cells visualized by fluorescence resonance energy transfer (FRET) microscopy. *Curr. Biol.* 10:1395–1398.

Stryer, L. 1978. Fluorescence energy transfer as a spectroscopic ruler. *Annu. Rev. Biochem.* 47:819–846.

Tsien, R. Y. 1998. The green fluorescent protein. *Annu. Rev. Biochem.* 67:509–544.

Wei, S. K., J. F. Quigley, S. U. Hanlon, B. O'Rourke, and M. C. Haigney. 2002. Cytosolic free magnesium modulates Na/Ca exchange currents in pig myocytes. *Cardiovasc. Res.* 53:334–340.